Research Article **Open Access**

Physical, Thermal and Spectroscopical Characterization of Biofield Treated Triphenylmethane: An Impact of Biofield Treatment

Trivedi MK[1], Branton A[1], Trivedi D[1], Nayak G[1], Bairwa K[2] and Jana S[2]*

[1]*Trivedi Global Inc., 10624 S Eastern Avenue Suite A-969, Henderson, NV 89052, USA*
[2]*Trivedi Science Research Laboratory Pvt. Ltd., Hall-A, Chinar Mega Mall, Chinar Fortune City, Hoshangabad Rd., Bhopal, Madhya Pradesh, India*

Abstract

Triphenylmethane is a synthetic dye used as antimicrobial agent and for the chemical visualization in thin layer chromatography of higher fatty acids, fatty alcohols, and aliphatic amines. The present study was an attempt to investigate the impact of biofield treatment on physical, thermal and spectroscopical chareacteristics of triphenylmethane. The study was performed in two groups i.e., control and treatment. The treatment group subjected to Mr. Trivedi's biofield treatment. The control and treated groups of triphenylmethane samples were characterized using X-ray diffraction (XRD), surface area analyzer, differential scanning calorimetry (DSC), thermogravimetric analysis (TGA), Fourier transform infrared (FT-IR), ultraviolet-visible (UV-Vis) spectroscopy, and gas chromatography-mass spectrometry (GC-MS). XRD study revealed decreases in average crystallite size (14.22%) of treated triphenylmethane as compared to control sample. Surface area analysis showed a slight increase (0.42%) in surface area of treated sample with respect to control. DSC thermogram of treated triphenylmethane showed the slight increase in melting point and latent heat of fusion with respect to control. TGA analysis of control triphenylmethane showed weight loss by 45.99% and treated sample showed weight loss by 64.40%. The T_{max} was also decreased by 7.17% in treated sample as compared to control. The FT-IR and UV spectroscopic result showed the similar pattern of spectra. The GC-MS analysis suggested a significant decrease in carbon isotopic abundance (expressed in $\delta^{13}C$, ‰) in treated sample (about 380 to 524‰) as compared to control. Based on these results, it is found that biofield treatment has the impact on physical, thermal and carbon isotopic abundance of treated triphenylmethane with respect to control.

Keywords: Triphenylmethane; Biofield treatment; X-ray diffraction; Differential scanning calorimetry; Thermogravimetric analysis; Gas chromatography-Mass Spectrometry (GC-MS)

Abbreviations

XRD: X-ray diffraction; DSC: Differential scanning calorimetry; TGA: Thermogravimetric analysis; DTA: Differential thermal analysis; FT-IR: Fourier transform infrared; UV-Vis: Ultraviolet-visible; GC-MS: Gas chromatography-mass spectrometry; PM: Primary molecule

Introduction

Triphenylmethane is a hydrocarbon with molecular formula $(C_6H_5)_3CH$. It builds the basic skeleton of many synthetic dyes such as bromocresol green, malachite green etc., and used as pH indicator and fluorescence agent [1]. Boulos RA has reported its antimicrobial property [2]. Triphenylmethane reported to inhibit 3-methyl-cholanthrene-induced neoplastic transformation of 10T1/2 cells in a dose-dependent manner and as a novel chemo preventive agent [3]. This has been used as visualizing agent in thin-layer chromatography of higher chain fatty acids, fatty alcohols, and aliphatic amines [4]. Recently, triphenylmethane was reported as an alternative for mediated electronic transfer systems in glucose oxidase biofuel cells (enzymatic biofuel cell). The enzymatic biofuel cell is a type of fuel cell wherein the enzymes are used as a catalyst to oxidize its fuel, instead of costly metals [5]. Hugle et al. used triphenylmethane as a possible moderator material to reduces the speed of neutrons in nuclear chain reactions, especially promising as cold neutrons moderator. It has a unique structure i.e., three aromatic phenyl groups surrounding one central carbon atom that is able to generate a stable radical ion [6]. Diverse applications of triphenylmethane especially as florescent indicator, mediator in biofuel and as a moderator had been suggested the importance of physicochemical property of triphenylmethane. It was previously reported that physical and thermal properties of molecule also affect its reactivity [7,8]. Hence, it is beneficial to find out an alternate approach that can improved the physicochemical properties of compounds like triphenylmethane, which can enhance its usability. Recently, biofield treatment reported to alter the spectral properties of various pharmaceutical drugs like chloramphenicol and tetracycline, and physicochemical properties of metals, beef extract and meat infusion powder [9-11].

Relation between mass and energy ($E=mc^2$) is well reported in literature [12]. The mass (solid matter) is consist of energy and when this energy vibrates at a certain frequency, it provides physical, atomic and structural properties like size, shape, texture, crystal structure, and atomic weight to the matter [13]. Similarly, human body also consists with vibratory energy particles like protons, neutrons, and electrons [14]. Due to vibrations in these particles, an electrical impulse is generated that cumulatively forms electromagnetic field, which is known as biofield [15]. The human has the ability to harness the energy from the environment or Universe and transmit this energy into any object (living or nonliving) on the Globe. The object(s) receive the energy and respond into useful way, this process is known as biofield treatment.

Mr. Trivedi's unique biofield energy is also called as The Trivedi Effect®, and reported to change various physicochemical, thermal and structural properties of several metals [10,16,17] and ceramics [18]. In addition, biofield treatment has been extensively studied in different fields such as agricultural science [19,20], biotechnology research [21], and microbiology research [22-24].

Conceiving the impact of biofield treatment on various living and nonliving things, the study aimed to evaluate the impact of biofield treatment on spectral and physicochemical properties of triphenylmethane using different analytical techniques.

Materials and Methods

Study design

Triphenylmethane was procured from Sisco Research Laboratories, India. The study was performed in two groups i.e., control and treatment. The control sample was remained as untreated; and treatment sample was handed over in sealed pack to Mr. Trivedi for biofield treatment under laboratory conditions. Mr. Trivedi provided the biofield treatment through his energy transmission process to the treatment group without touching the sample [9]. The control and treated samples of triphenylmethane were evaluated using various analytical techniques like X-ray diffraction (XRD), surface area analyzer, differential scanning calorimetry (DSC), thermogravimetric analysis (TGA), Fourier transform infrared (FT-IR), ultraviolet-visible (UV-Vis) spectroscopy, and gas chromatography-mass spectrometry (GC-MS).

X-ray diffraction (XRD) study

XRD analysis of triphenylmethane was performed on Phillips, Holland PW 1710 X-ray diffractometer with copper anode and nickel filter. Wavelength of X-ray used in XRD system was 1.54056 Å with scanning rate of 0.05° 2/s, and a chart speed of 10 mm/2. Data obtained from XRD system were in the form of a chart of 2θ (10-100°) *vs.* intensity. The average crystallite size (G) of triphenylmethane was calculated using the following equation [25].

$$G = k\lambda/(bCos\theta)$$

Percent change in average crystallite size = $[(G_t-G_c)/G_c] \times 100$

Where, G_c and G_t are average crystallite size of control and treated powder samples respectively.

Surface area analysis

Surface area of control and treated triphenylmethane was measured using the Brunauer–Emmett–Teller (BET) surface area analyzer, Smart SORB 90. Percent changes in surface area were calculated using following equation:

$$\% \text{ change in surface area} = \frac{[S_{Treated} - S_{Control}]}{S_{Control}} \times 100$$

Where, $S_{Control}$ and $S_{Treated}$ are the surface area of control and treated samples, respectively.

Differential scanning calorimetry (DSC) study

The control and treatment samples of triphenylmethane were analyzed using a Pyris-6 Perkin Elmer differential scanning calorimeter (DSC) on a heating rate of 10°C/min under air atmosphere with air flow rate of 5 mL/min. An empty pan sealed with covered aluminum pan was used as a reference. The melting temperature (T_m) and latent heat of fusion (ΔH) were obtained from the DSC curve.

Thermogravimetric analysis-differential thermal analysis (TGA-DTA)

Thermal stability of control and treated triphenylmethane were analyzed using Mettler Toledo simultaneous TGA and differential thermal analyzer (DTA). The samples were heated from room temperature to 400°C with a heating rate of 5°C/min under air atmosphere. Percent change in temperature at which maximum weight loss occurs in sample was calculated.

Spectroscopic studies

For determination of FT-IR and UV-Vis spectroscopic characters, the treated sample was divided into two groups i.e., T1 and T2. Both treated groups were analyzed for their spectral characteristics using FT-IR and UV-Vis spectroscopy as compared to control triphenylmethane sample. While, for GC-MS analysis, the treated sample was divided into four groups i.e., T1, T2, T3, and T4 and all treated groups were analyzed along with control sample for isotopic abundance of carbon-13.

FT-IR spectroscopic characterization

FT-IR spectra of control and treated samples of triphenylmethane were recorded on Shimadzu's Fourier transform infrared spectrometer (Japan) with frequency range of 4000-500 cm⁻¹. The analysis was accomplished to evaluate the effect of biofield treatment at atomic level like dipole moment, force constant and bond strength in chemical structure [26].

UV-Vis spectroscopic analysis

UV spectra of control and treated samples of triphenylmethane were obtained from Shimadzu UV-2400 PC series spectrophotometer. A quartz cell with 1 cm and a slit width of 2.0 nm was used for analysis. The study was carried out using wavelength in the range of 200-400 nm. The UV spectra were analyzed to determine the effect of biofield treatment on the energy gap of bonding and nonbonding transition of electrons [26].

Gas chromatography-mass spectroscopy (GC-MS) analysis

The GC-MS analysis of control and treatment samples (T1, T2, T3, and T4) of triphenylmethane were performed on Perkin Elmer/auto system XL with Turbo mass and electron ionization mode, USA. Detection limit was set to 1 Pico gram, and mass range was set to 10-650 amu. The isotopic ratio ¹³C/¹²C was expressed by its deviation in treated triphenylmethane sample with respect to control. The isotopic abundance of ¹³C was computed on a delta scale per thousand. The values of δ¹³C of treated samples were calculated using following equation [27].

$$\delta^{13}C (\text{‰}) = \frac{R_{Treated} - R_{Control}}{R_{Control}} \times 1000 \quad (1)$$

Where, $R_{Treated}$ and $R_{Control}$ are the ratio of intensity at *m/z*=245/*m/z*=244 for δ¹³C in mass spectra of treated and control samples respectively.

Results and Discussion

XRD analysis

XRD of control and treated triphenylmethane are presented in Figure 1. The control triphenylmethane showed the XRD peaks at 2θ equals to 11.70°, 11.91°, 15.00°, 18.24°, 19.67°, 22.52°, 22.66°, 23.99°, 24.96°, 26.19°, and 28.71°. However, the XRD diffractogram of treated triphenylmethane showed the decrease in intensity of the peaks. XRD peaks in treated sample were appeared at 2θ equals to 11.92°, 12.33°, 14.87°, 15.03°, 18.25°, 19.66°, 20.76°, 22.52°, 23.99°, 24.24°, and 26.19°.
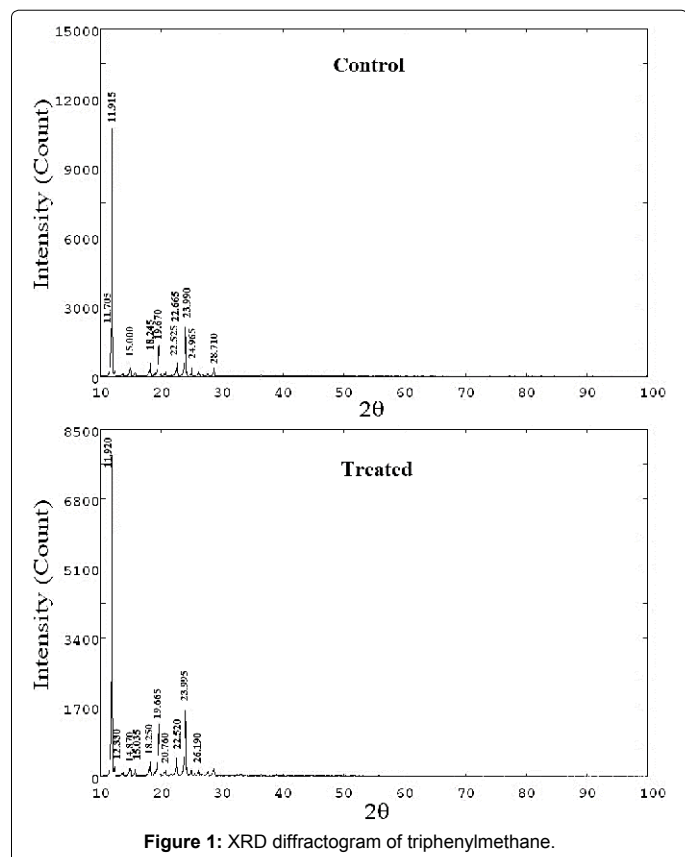
Figure 1: XRD diffractogram of triphenylmethane.

The sharp and intense peak in XRD diffractogram of control and treated samples suggested the crystalline nature of triphenylmethane in both samples. The result showed that the XRD peaks were shifted after biofield treatment as 1191°→1192°; 1500°→15.03°; 18.24°→18.25°; 19.67°→19.66°; 24.96°→24.24° etc. moreover, few peaks like 11.70° and 28.7° in control sample are disappeared or their intensity is decreased after biofield treatment. The decrease in intensity of XRD peaks in biofield treated triphenylmethane might be attributed to decrease in long-range order of the molecules. The average crystallite size was calculated using Scherrer formula and the result are shown in Figure 2. The average crystallite size of control triphenylmethane was found as 117.17 nm that was decreased to 100.51 nm in treated sample. The result showed about 14.22% decrease in average crystallite size in treated sample as compared to control. It was reported that increase in internal micro strain leads to decrease the corresponding crystallite size of the material [27]. Moreover, Zhang et al. showed that presence of strain and increase atomic displacement from their ideal lattice positions causes reduction in crystallite size [28]. Hence, it is assumed that biofield treatment may induce the internal strain in triphenylmethane. This might be the responsible for decrease in average crystallite size of the treated triphenylmethane as compared to control.

Surface area analysis

The surface area of control and treated samples of triphenylmethane was determined using BET surface area analyzer and data are presented in Figure 3. The control sample showed a surface area of 0.8243 m^2/g; however, the treated sample of triphenylmethane showed a surface area of 0.8278 m^2/g. The result showed a slight increase in surface area (0.42%) in the treated triphenylmethane sample as compared to control. The increase in surface area might be correlated to particle size reduction due to high internal strain produced by biofield treatment

[29]. The increase in surface area may lead to increase in solubility [30] and reactivity of triphenylmethane as compared to control.

DSC analysis

DSC was used to analyze the melting temperature and latent heat of fusion (ΔH) of control and treated triphenylmethane. In solid materials, substantial amount of interacting forces exist in atomic level that hold the atoms at their positions. ΔH is defined as the energy needed to overcome the interaction force to change the solid phase into liquid phase. Hence, the energy provided during phase change i.e., ΔH is stored as potential energy of atoms. However, melting point is related with kinetic energy of the atoms [31]. DSC thermogram showed the melting temperature at 94.57°C in control and 95.11°C in treated sample (Table 1), which revealed about 0.57% increase in melting temperature in treated sample of triphenylmethane with respect to control. The melting temperature of triphenylmethane was well supported by literature data [32]. Likewise, the DSC thermogram exhibited the latent heat of fusion i.e., 85.05 J/g in control and 85.27 J/g in treated sample of triphenylmethane. The result depicted about 0.26% change in latent heat of fusion of treated sample as compared to control.

Thermogravimetric analysis (TGA)/derivative thermogravimetry (DTG) analysis

The TGA and DTG analysis of control and treated samples of triphenylmethane are shown in Table 1. TGA thermogram of control triphenylmethane exhibited the onset temperature around 216.00°C that was end-set around 257.00°C with 45.99% weight loss. However, the treated triphenylmethane started losing weight around 193.00°C and end-set around at 248.00°C with 64.40% weight loss (Figure 4). The result showed decrease in onset temperature of treated triphenylmethane by 10.65% as compared to control. Moreover, DTG thermogram exhibited the maximum thermal decomposition
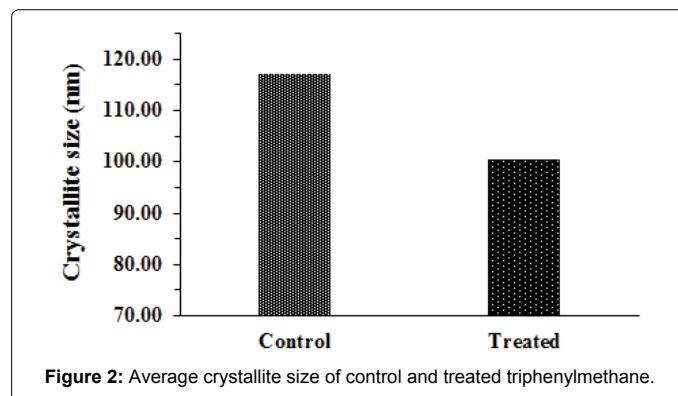

Figure 2: Average crystallite size of control and treated triphenylmethane.
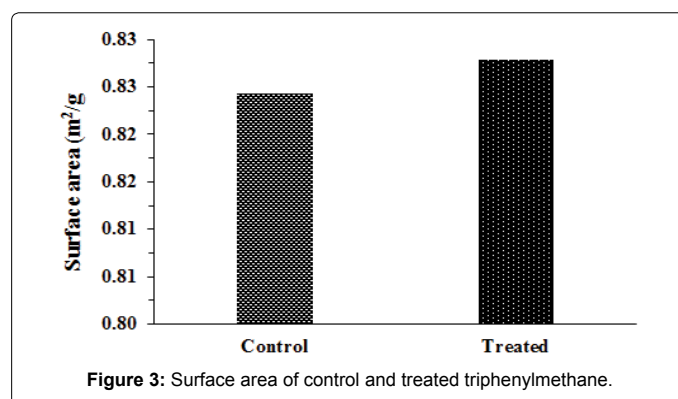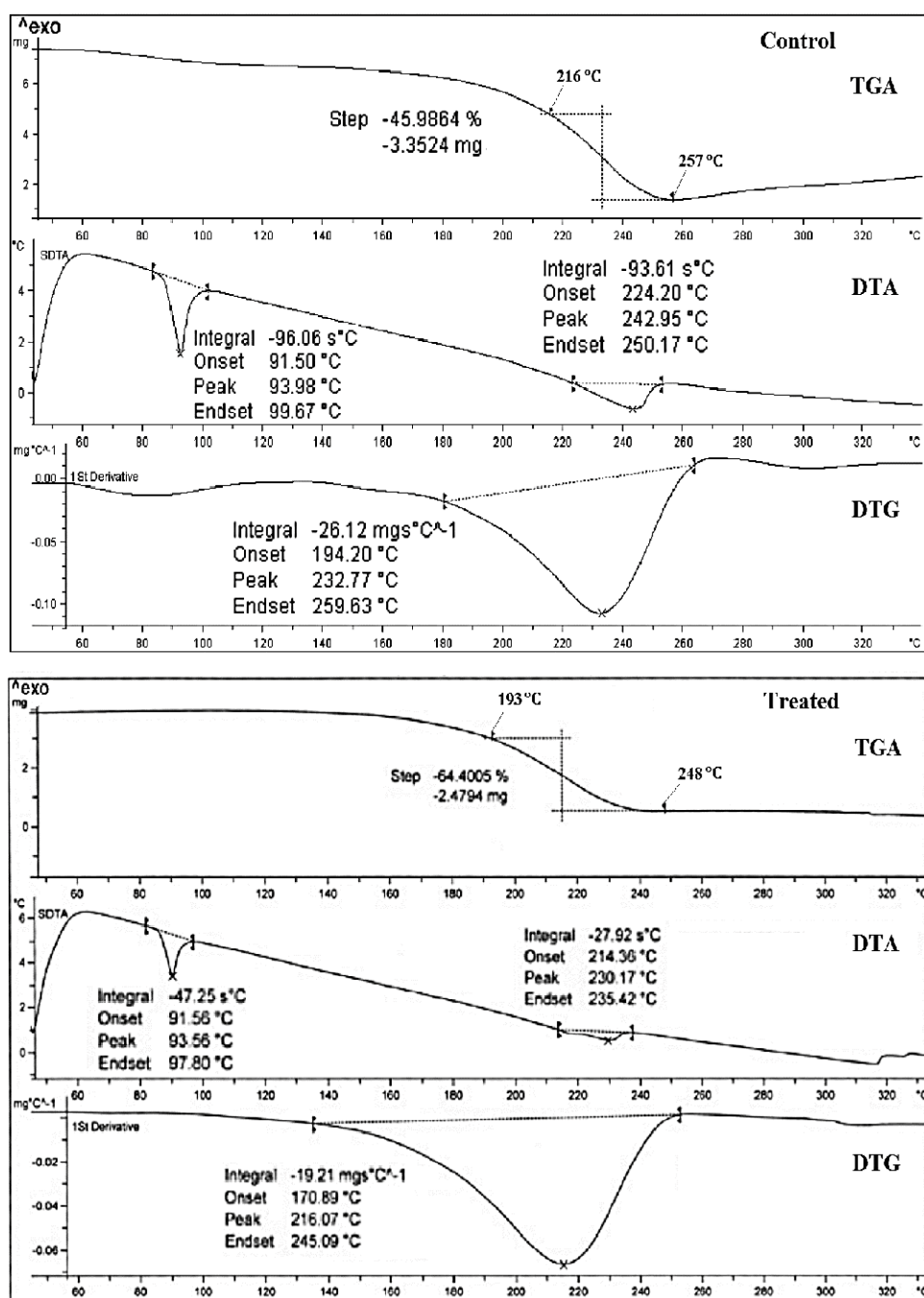

Figure 3: Surface area of control and treated triphenylmethane.

temperature (T_{max}) at 232.77°C in control sample and at 216.07°C in treated sample of triphenylmethane. The result suggested about 7.17% decrease in T_{max} of treated sample with respect to control. The decrease in T_{max} of treated sample might be correlated with increase in vaporization or volatilization of treated triphenylmethane after biofield treatment. It might be due to alteration in internal energy that results into earlier vaporization of treated triphenylmethane sample as compared to control.

S No	Parameter	Control	Treated
1	Latent heat of fusion (J/g)	85.05	85.27
2	Melting point (°C)	94.57	95.11
3	Onset temperature (°C)	216.00	193.00
4	T_{max} (°C)	232.77	216.07

Table 1: Thermal analysis of control and treated samples of triphenylmethane. T_{max}: Temperature at maximum weight loss occurs.

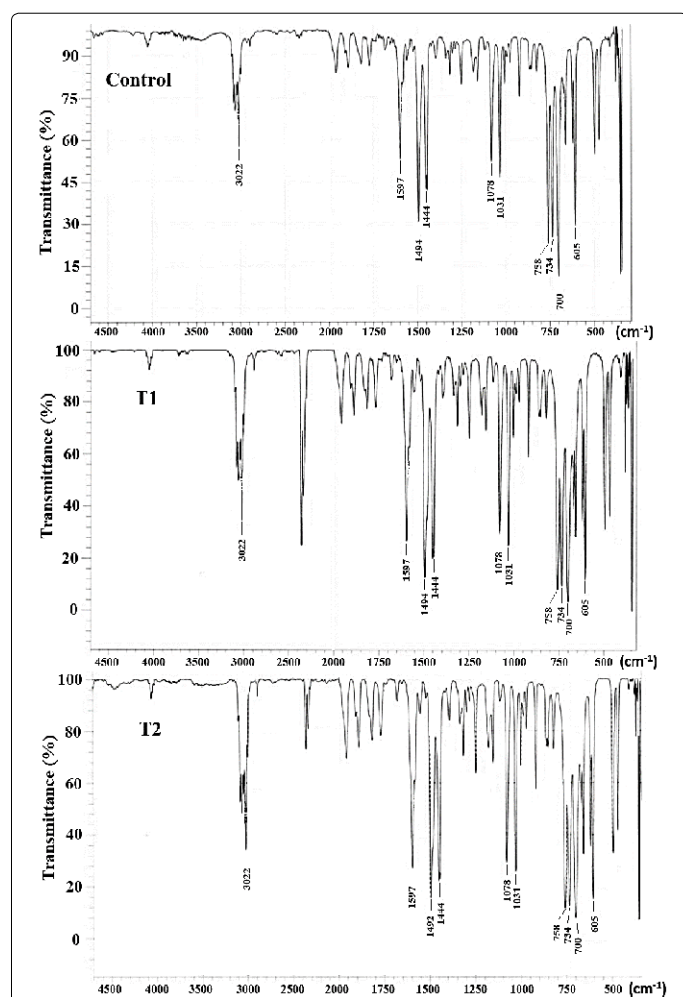**Figure 4:** TGA thermogram of control and treated triphenylmethane.

Figure 5: FT-IR spectra of control and treated (T1 and T2) triphenylmethane.

Wave number (cm⁻¹)			Frequency assigned
Control	T1	T2	
3022	3022	3022	C-H stretching
1444-1597	1444-1597	1444-1597	C=C stretching
1031-1078	1031-1078	1031-1078	C-H in-plane deformation
605-758	605-758	605-758	C-H out of plane deformation

Table 2: FT-IR Spectral analysis of triphenylmethane.

FT-IR spectroscopic analysis

The recorded FT-IR spectra (Figure 5) were analyzed based on theoretically predicted wavenumber and presented in Table 2. The chemical structure of triphenylmethane consists with three phenyl groups attached with a methyl carbon. Therefore, The FT-IR spectra of triphenylmethane should contains the stretching and bending peaks mainly due to C-H and C=C groups. The C-H stretching was assigned to peak appeared at 3022 cm⁻¹ in control and treated (T1 and T2) samples. The C=C stretchings of phenyl ring carbon were assigned to vibrational peak observed at 1444-1597 cm⁻¹ in all three samples i.e., control, T1, and T2. The C-H in-plane deformation peaks were attributed to vibrational peaks observed at 1031-1078 cm⁻¹ in all three samples i.e., control, T1, and T2. In addition, the C-H out of plane deformation peaks were assigned to IR peak appeared at 605-758 cm⁻¹ in control, T1, and T2 samples. The FT-IR spectrum of triphenylmethane was well supported with the literature data [33]. The FT-IR result suggested

that the biofield treatment did not induce any structural changes in the triphenylmethane sample with respect to control.

UV-Vis spectroscopy

UV spectrum of control triphenylmethane showed absorbance maxima (λ_{max}) at 207.0, 262.0 and 269.4 nm. Similar pattern of λ_{max} was observed for both the treated samples (T1 and T2) i.e., at 213.0, 261.8, and 269.2 nm in T1 and 206.5, 261.5, and 269.0 nm in T2. The result exhibited a slight bathochromic shift of peak at 213.0 nm in T1 as compared to control (207.0 nm). Apart from this, other peaks were observed at the similar wavelength in all three samples i.e., control, T1 and T2. Overall, the UV spectral analysis suggests that biofield treatment did not cause any significant alterations in the λ_{max} of treated molecules as compared to control. The findings of UV analysis were also supported by the FT-IR results.

GC-MS analysis

The GC-MS spectra of control and treated (T1, T2, T3, and T4) samples of triphenylmethane are shown in Figures 6a and 6b, and the peak intensity of molecular ion and most probable isotopes are illustrated in Table 3. The GC-MS spectra of control and treated samples showed the primary molecule (PM, triphenylmethane) peak at m/z 244, which suggested the molecular weight of triphenylmethane. In addition, the peak at m/z 245 was assigned to isotopic abundance peaks due to PM^{+1} (^{13}C/^{12}C). It is assumed that isotopic abundance ratio of PM^{+1} was mainly due to ^{13}C and ^{2}H isotopes in triphenylmethane. Based on this, it is speculated that the peak at m/z 244 is may be due to
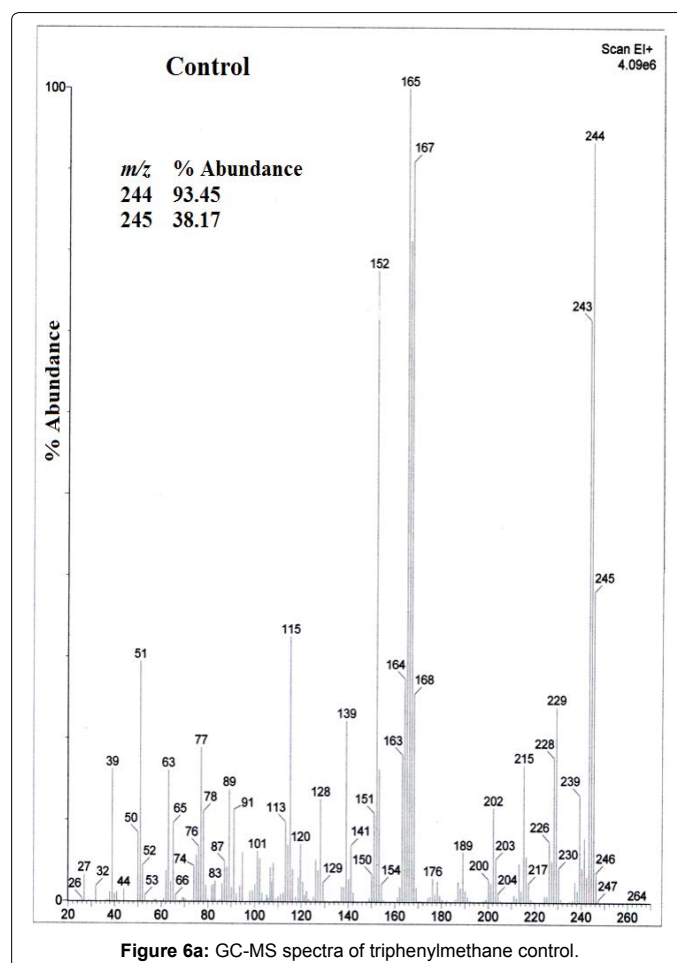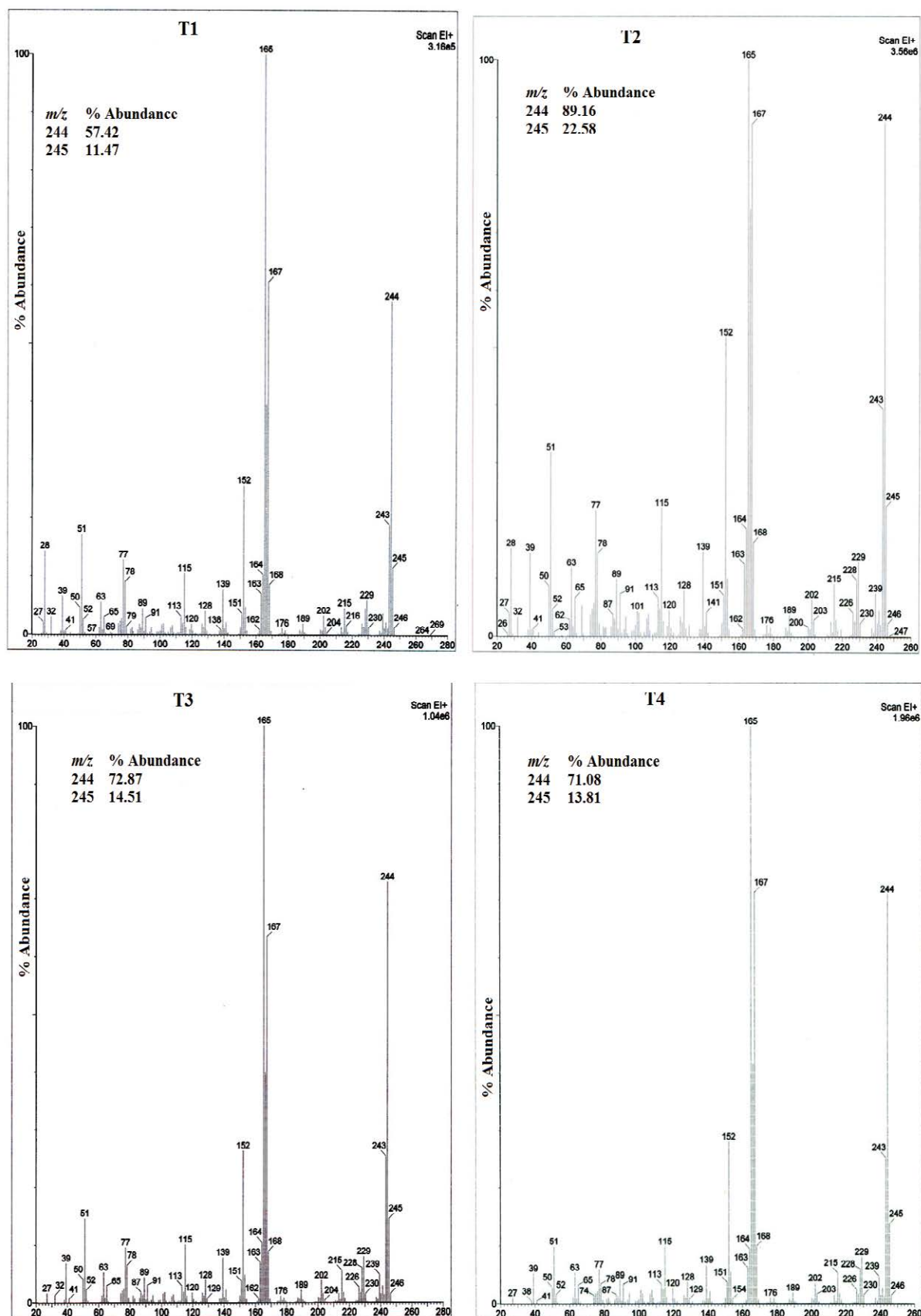

Figure 6a: GC-MS spectra of triphenylmethane control.

Figure 6b: GC-MS spectra of triphenylmethane (T1, T2, T3 and T4).

Parameter	Control	Treated			
		T1	T2	T3	T4
Peak intensity at m/z=244 (PM)	93.45	57.42	89.16	72.87	71.08
Peak intensity at m/z=245 (PM^{+1})	38.17	11.47	22.58	14.51	13.81
Ration of peak intensity [(100 × (PM^{+1}/PM)]	40.845	19.976	25.325	19.912	19.429
Carbon isotopic abundance (δ^{13}C ‰) with respect to control		-510.9	-380.0	-512.5	-524.3

Table 3: GC-MS isotopic abundance analysis of triphenylmethane. PM: Primary molecule (triphenylmethane).

$^{12}C_{19}{}^{1}H_{16}$ and m/z 245 is due to $^{13}C_{1}{}^{12}C_{18}{}^{1}H_{16}$ and $^{12}C_{19}{}^{2}H_{1}{}^{1}H_{15}$. The GC-MS analysis result (Table 3) showed that carbon isotopic abundance (expressed in δ^{13}C, ‰) was changed as -510.9, -380.0, -512.5, and -524.3‰ in T1, T2, T3, and T4, respectively with respect to control. The result depicted that in the entire treated samples (T1, T2, T3, and T4) the ^{13}C and ^{2}H were transformed into ^{12}C and ^{1}H by releasing a neutron from their higher isotopes. This conversion of $^{13}C \rightarrow {}^{12}C$ and $^{2}H \rightarrow {}^{1}H$ might be possible if a nuclear level reaction occurred due to influence of biofield treatment. Based on this, it is postulated that biofield treatment possibly induced the nuclear level reactions in triphenylmethane, which may lead to convert the ^{13}C into ^{12}C and ^{2}H into ^{1}H in treated sample as compared to control.

Conclusions

XRD diffractogram of biofield treated triphenylmethane showed the alteration in intensity of XRD peaks and average crystallite size (14.22%) as compared to control. The surface area analysis showed the slight increase in surface area of treated triphenylmethane with respect to control. The thermal analysis (DSC, TGA/DTG) showed a slight change in melting temperature and latent heat of fusion in treated triphenylmethane as compared to control. The T_{max}, was also decreased by 7.17% in treated sample as compared to control. The spectroscopic analysis (FT-IR and UV-Vis) showed that biofield treatment did not affect the dipole moment, bond force constant and the absorbance maxima (λ_{max}) of treated sample as compared to control. GC-MS analysis showed the alteration in carbon isotopic abundance (δ^{13}C) as -510.9, -380.0, -512.5, and -524.3‰ in T1, T2, T3, and T4, respectively as compared to control.

Overall, the physical, thermal and spectroscopical study suggests the impact of biofield treatment on physicochemical properties of treated triphenylmethane with respect to control. Based on this it is assumed that treated triphenylmethane could be more useful as compared to control.

Acknowledgements

References

1. Kolling OW, Smith ML (1959) Selected triphenylmethane dyes as acid-base indicators in glacial acetic acid. Anal Chem 31: 1876-1879.

2. Boulos RA (2013) Antimicrobial dyes and mechanosensitive channels. Antonie Van Leeuwenhoek 104: 155-167.

3. Cooney RV, Pung A, Harwood PJ, Boynton AL, Zhang LX, et al. (1992) Inhibition of cellular transformation by triphenylmethane: a novel chemopreventive agent. Carcinogenesis 13: 1107-1112.

4. Kwapniewski Z, Cichon R (1979) The application of triphenylmethane dyes to visualization of selected aliphatic compounds in thin-layer chromatography. Microchem J 24: 298-299.

5. La Rotta H CE, Ciniciato GP, González ER (2011) Triphenylmethane dyes, an alternative for mediated electronic transfer systems in glucose oxidase biofuel cells. Enzyme Microb Technol 48: 487-497.

6. Hugle T, Mocko M, Hartl MA, Daemen LL, Muhrer G (2014) Triphenylmethane, a possible moderator material. Nucl Instrum Methods Phys Res A 738: 1-5.

7. Carballo LM, Wolf EE (1978) Crystallite size effects during the catalytic oxidation of propylene on ^{Pt}/γ-Al$_2$O$_3$. J Catal 53: 366-373.

8. Chaudhary AL, Sheppard DA, Paskevicius M, Pistidda C, Dornheim M, et al. (2015) Reaction kinetic behaviour with relation to crystallite/grain size dependency in the Mg-Si-H system. Acta Mater 95: 244-253.

9. Trivedi MK, Patil S, Shettigar H, Bairwa K, Jana S (2015) Spectroscopic characterization of chloramphenicol and tetracycline: An impact of biofield. Pharm Anal Acta 6: 1-5.

10. Trivedi MK, Patil S, Tallapragada RM (2013) Effect of bio field treatment on the physical and thermal characteristics of silicon, tin and lead powders. J Material Sci Eng 2: 1-7.

11. Trivedi MK, Nayak G, Patil S, Tallapragada RM, Jana S, et al. (2015) Bio-field treatment: An effective strategy to improve the quality of beef extract and meat infusion powder. J Nutr Food Sci 5: 389.

12. Einstein A (1905) Does the inertia of a body depend upon its energy-content? Ann Phys 18: 639-641.

13. Becker RO, Selden G (1985) The body electric: Electromagnetism and the foundation of life. New York City, William Morrow and Company.

14. BARNES RB (1963) Thermography of the human body. Science 140: 870-877.

15. Rubik B (2002) The biofield hypothesis: its biophysical basis and role in medicine. J Altern Complement Med 8: 703-717.

16. Trivedi MK, Tallapragada RR (2008) A transcendental to changing metal powder characteristics. Met Powder Rep 63: 22-28.

17. Trivedi MK, Patil S, Tallapragada RM (2012) Thought intervention through biofield changing metal powder characteristics experiments on powder characterisation at a PM Plant. Future Control and Automation LNEE 173: 247-252.

18. Trivedi MK, Patil S, Tallapragada RM (2013) Effect of biofield treatment on the physical and thermal characteristics of vanadium pentoxide powders. J Material Sci Eng S11: 001.

19. Sances F, Flora E, Patil S, Spence A, Shinde V (2013) Impact of biofield treatment on ginseng and organic blueberry yield. Agrivita J Agric Sci 35.

20. Lenssen AW (2013) Biofield and fungicide seed treatment influences on soybean productivity, seed quality and weed community. Agricultural Journal 8: 138-143.

21. Patil SA, Nayak GB, Barve SS, Tembe RP, Khan RR (2012) Impact of biofield treatment on growth and anatomical characteristics of Pogostemon cablin (Benth.). Biotechnology 11: 154-162.

22. Trivedi MK, Patil S (2008) Impact of an external energy on Staphylococcus epidermis [ATCC-13518] in relation to antibiotic susceptibility and biochemical reactions-an experimental study. J Accord Integr Med 4: 230-235.

23. Trivedi MK, Patil S (2008) Impact of an external energy on Yersinia enterocolitica [ATCC-23715] in relation to antibiotic susceptibility and biochemical reactions: an experimental study. Internet J Alternat Med 6: 1-6.

24. Trivedi MK, Patil S, Shettigar H, Gangwar M, Jana S (2015) Antimicrobial sensitivity pattern of Pseudomonas fluorescens after biofield treatment. J Infect Dis Ther 3: 222.

25. Patterson AL (1939) The Scherrer formula for X-Ray particle size determination. Phys Rev 56: 978-982.

26. Pavia DL, Lampman GM, Kriz GS (2001) Introduction to spectroscopy. 3rd edn, Thomson Learning, Singapore.

27. Paiva-Santos CO, Gouveia H, Las WC, Varela JA (1999) Gauss-Lorentz size-strain broadening and cell parameters analysis of Mn doped SnO$_2$ prepared by organic route. Mat Structure 6: 111-115.

28. Zhang K, Alexandrov IV, Kilmametov AR, Valiev RZ, Lu K (1997) The crystallite-size dependence of structural parameters in pure ultrafine-grained copper. J Phys D Appl Phys 30: 3008-3015.

29. Trivedi MK, Nayak G, Tallapragada RM, Patil S, Latiyal O, et al. (2015) Effect of biofield treatment on structural and morphological properties of silicon carbide. J Powder Metall Min 4: 1-4.

30. Hansen CM (2007) Hansen Solubility Parameters: A User's Handbook. 2nd edn, CRC press.

31. Jamin E, Martin F, Martin GG (2004) Determination of the 13C/12C ratio of ethanol derived from fruit juices and maple syrup by isotope ratio mass spectrometry: collaborative study. J AOAC Int 87: 621-631.

32. Cornish hh, Zamora E, Bahor RE (1964) Metabolism of Triphenylmethane and Triphenylcarbinol. Arch Biochem Biophys 107: 319-324.

33. Cheriaa J, Khaireddine M, Rouabhia M, Bakhrouf A (2012) Removal of triphenylmethane dyes by bacterial consortium. ScientificWorld Journal 2012: 512454.